A Study of Time Variations in the Cosmic-Ray Directional Intensity Distribution*

MAX L. YEATER†
Department of Physics, Washington University, St. Louis, Missouri
(Received October 13, 1944)

Evidence of time variations in the cosmic-ray directional intensity distribution has been obtained, by a statistical analysis of directional intensity measurements carried out at St. Louis in 1943. The variations, occurring within periods of twelve to twenty-eight hours, seem most pronounced near zenith angles of $\pm 20°$ and $\pm 70°$ in the east–west plane, and are not found in the north–south plane. These observations would appear to be explained by the effect of terrestrial magnetic fluctuations in modifying the allowed cones of certain primary cosmic-ray particles, these particles having energies grouped near 0.2 Störmer and 0.6 Störmer. If this hypothesis is correct, the east–west positional symmetry of these variations constitutes new evidence, supporting previous evidence of Schremp, that positive and negative particles with the same e/m exist in the *primary* cosmic radiation. Earlier results of Ribner, Cooper, and Schremp, on the static fine structure pattern of cosmic-ray directional intensity, are also supported by the present data. The time variations in the intensity distribution reported here are variations in the fine structure pattern, but appear to be independent of the static prominences previously reported. The method for rapid exploration of the cosmic-ray directional intensity distribution is described. The multidirectional cosmic-ray telescope used is discussed in some detail.

I. INTRODUCTION

FROM theoretical considerations, based on the theory of the allowed cone[1] and the theory of atmospheric absorption of cosmic rays, Schremp predicted[2,3] that a fine structure pattern should exist in the cosmic-ray directional intensity distribution, and indicated[4] how a study of this pattern should provide information concerning the nature, energy spectra, and absorptive properties of the primary cosmic rays. The actual existence of the fine structure has been established by experiments of Ribner[5] and Cooper[6] in Missouri, and of Schremp and Baños[7] in Mexico City.

In Missouri the fine structure pattern was observed to have a circular symmetry about the zenith. This was interpreted as indicating the existence of lines or bands in the primary energy spectra, for particles too energetic to be observably influenced by the earth's magnetic field.[8] At Mexico City one circular ring of prominences was observed, corroborating the results obtained in Missouri. Other prominences in the Mexico City pattern failed to exhibit this circular symmetry, but were nearly mirror images of one another in the N–S plane. The latter provided evidence that the primary radiation contains positive and negative particles with the same e/m.[9]

Although these experiments dealt with the static characteristics of the fine structure pattern, the existence of time variations in the pattern was suspected.[10] In spite of the realization that new information might be revealed by the study of these time variations,[11] the matter could not be pursued at that time because of limitations in apparatus. The first attempt to explore such cosmic-ray fine structure time variations, with new apparatus, is discussed in this paper.

II. APPARATUS

A directional detecting system with a high counting rate combined with high angular resolution is needed. The cosmic-ray telescope used in this experiment was designed to measure radia-

* From a dissertation submitted in partial fulfillment of the requirements for the Ph.D. degree at Washington University.
† Now at the Radiation Laboratory, Massachusetts Institute of Technology, Cambridge, Massachusetts.
[1] M. S. Vallarta, J. Frank. Inst. **227**, 1 (1939) (summary); E. J. Schremp, Phys. Rev. **54**, 157 (1938); R. Albagli Hutner, Phys. Rev. **55**, 15 and 614 (1939).
[2] E. J. Schremp, Phys. Rev. **53**, 915A (1938).
[3] E. J. Schremp, Phys. Rev. **54**, 157 (1939).
[4] E. J. Schremp and H. S. Ribner, Rev. Mod. Phys. **11**, 149 (1939).
[5] H. S. Ribner, Phys. Rev. **56**, 1069 (1939).
[6] D. M. Cooper, Phys. Rev. **58**, 288 (1940).
[7] E. J. Schremp and Alfredo Baños, Jr., Phys. Rev. **59**, 614 (1941).
[8] See reference 4, p. 150.
[9] Cf. reference 7.
[10] Cf. references 4–6.
[11] Cf. references 4–6.

tion from eighteen directions simultaneously, using fairly large Geiger counters and large spacings between counters. The cross section for each of the directional systems is about 2.5 square feet. The dimensions are so adjusted that the geometrical angular aperture for any direction is 7° 40′ in the plane of the drum and 18° 18′ in the plane of the counter anode wires.

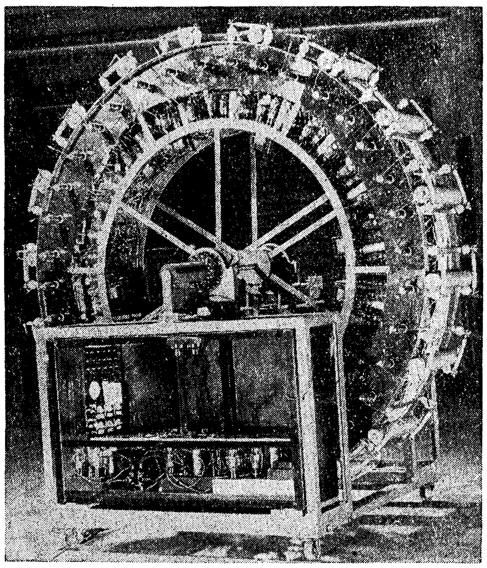

FIG. 1. Multidirectional cosmic-ray telescope. At the time this picture was taken only eighteen of the seventy-two Geiger counters were in position on the drum.

The use of this equipment, which is described in detail below, has indicated how certain improvements in apparatus would enable one to secure more complete information from this type of experiment. A summary of these suggested improvements in apparatus is included in Appendix III.

1. The Geiger-Müller Counters

The type of counter used is essentially that recommended by Trost,[12] consisting of a brass cathode, a tungsten anode, and a filling of argon plus organic vapor. A departure from conventional counter construction lies in the elimination of the usual glass envelope. The filling gas includes a mixture of alcohol and petroleum ether which minimizes temperature effects in the counting rate.

Further details of the Geiger counters are given in Appendix I.

2. Mechanical Arrangement of Telescope

The multidirectional cosmic-ray telescope is shown in Fig. 1. The Geiger-Müller counters are mounted on the outer periphery of a drum six feet in diameter. One Neher-Pickering quenching circuit is provided for each set of counters; these circuits are mounted on a side panel which circles the drum on one side just below the counters. Shielded cables, encircling the drum in a layer beneath the counters, distribute pulses from the quenching circuits to the mixing circuits, which are below the cables. The high voltage power supplies are in a cabinet built into the base; the eighteen message registers which record the impulses for the eighteen directions are also in this cabinet. Slip rings and brushes link the circuits on the drum and in the cabinet. In the cabinet all the meters are on one panel; a movie camera is set up to photograph this panel automatically.

Changing the azimuth in which the plane of the drum lies can only be accomplished by moving the whole structure of the telescope. The zenith angle, however, can be changed automatically. The drive for this is provided by a $\frac{1}{8}$-hp, 1725-r.p.m. G.E. motor, with a 900:1 Boston "Reductor" and a 60:1 worm and gear. The automatic control circuit, for the drum and the camera, is in the cabinet with the power supplies.

3. Electric Circuits

a. Automatic Control Circuit

This circuit carries out these functions: It automatically starts the motor at periodic time intervals of twenty minutes, thirty minutes or one hour, and automatically stops the motor when the drum has rotated through a predetermined angular interval of one, three, or six degrees; it operates a message register which indicates the new position of the drum after the rotation, and automatically operates a camera to photograph the readings of the recording instruments at the end of the rotation of the drum. Provision is made for leaving the drum stationary and automatically photographing the instrument panel at intervals of twenty minutes, thirty minutes, or one hour.

[12] Adolf Trost, Zeits. f. Physik **105**, 399 (1937).

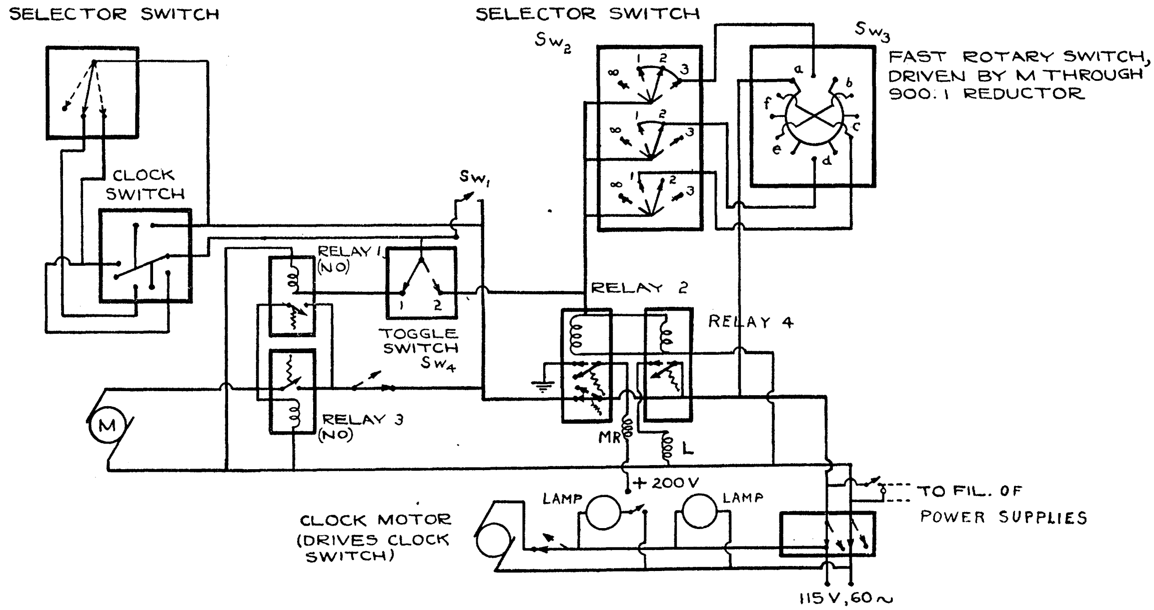

FIG. 2. Control circuit providing for automatic rotation of drum and photographing of meters in the multidirectional cosmic-ray telescope.

The essential features of this circuit, and the design of the special switch which makes this operation possible, have been described elsewhere;[13] a simplified circuit is given in this reference. Additional explanatory notes for the complete control circuit, which appears in Fig. 2, are given in Appendix IV.

b. Neher-Pickering Quenching Circuit

This is a conventional circuit; its operation is described elsewhere.[14] The constants are given in Fig. 3.

c. Mixing and Recording Circuit

This circuit, shown in Fig. 4, is a combination of the Rossi coincidence circuit[15] and the Johnson multivibrator circuit.[16] Its function is to accept pulses from five co-directional trains of counters (i.e., from the quenching circuits associated with these trains) and cause a message register to record a count whenever any one of these trains experiences a coincidence of cosmic-ray impulses in its members. The operation, briefly, is as follows: The 6C6 mixer tubes are normally conducting; whenever two negative pulses from counters on opposite sides of the drum come to the grids of any pair of the 6C6's, say A and B, the voltage across R_1' rises sharply and fires neon lamp Ne'. This causes the drop across R_2 to

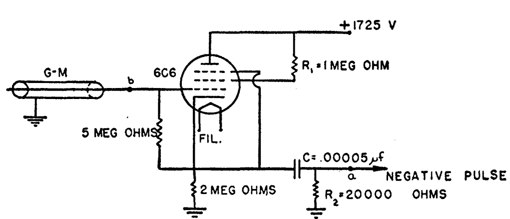

FIG. 3. Neher-Pickering quenching circuit.

[13] M. L. Yeater, Rev. Sci. Inst. **14**, 146 (1943).
[14] A. L. Hughes, Am. Phys. T. **7**, 271 (1939).
[15] B. Rossi, Nature **125**, 636 (1930).

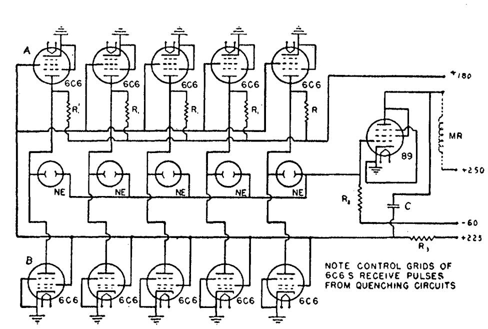

FIG. 4. Mixing and recording circuit for one direction; $R_1 = R_1' = 50{,}000$ ohms, $R_2 = 1$ megohm, $R_3 = 0.1$ megohm; Ne, $\frac{1}{4}$-watt neon lamps.

[16] T. H. Johnson, Rev. Sci. Inst. 9, 221 (1938).

change so that the 89, a power tube, conducts. The duration of the conducting state in the 89 is increased by the feedback through C so that the message register coil MR in the plate circuit of the 89 can operate a mechanical numbering device.

Eighteen such circuits are used, one for each direction for which cosmic-ray intensities are measured. These are mounted on separate panels which encircle the drum; they are visible in Fig. 1, and have been identified in the description already given for the mechanical arrangement of the cosmic-ray telescope. The pulses received by these circuits from the quenching circuits must be sorted by a system of feeder cables, so that each mixer tube receives pulses only from the proper quenching circuit. This cable system is described in Appendix II.

d. Power Supplies

The regulated power supply for the plates of the 6C6 tubes in the coincidence circuits follows the circuit of Fig. 5. The screens of these tubes are provided with a similar supply which is also used for the negative voltage for the bias of the 89 power tube. The third supply, which operates the message registers through the power tube in the recording circuit, also uses the same circuit; two 2A3's are used in parallel, however, and heavier transformer and choke are used, because of the larger current.

The circuit shown in Fig. 6 provides the high voltage for the Geiger-Müller counters. In the type of experiment here involved, where the apparatus must run continuously for weeks or months, the first requirement for the high voltage supply is that it exhibit no drift in output voltage. It was found desirable to take these precautions:

(1) In order to avoid possible changes in the grid voltage for the 6J7, in the regulator circuit, the usual potentiometer was not used lest a defective contact arise at a, Fig. 6, where a changing potential is normally the means of controlling the output voltage.

(2) Batteries were used in the cathode circuit of the 6J7, in the regulator; neon lamps were first tried but were not reliable.

(3) The vacuum tubes are all mounted in the upright position. The voltage becomes noticeably erratic if this is not done.

When these precautions were taken the drift amounted to 1.5 percent at most; some of this may have been meter drift. No ripple greater than one volt could be detected in the output by the oscillograph.

As an additonal precaution, the input to all power supplies came from heavy duty Sola constant voltage transformers.

4. Light and Temperature Sensitivity

A serious difficulty arose from the effect of light on the sensitivity of the system. A periodic daily change in counting rate was observed. This effect was traced to the neon lamps in the multivibrator recording circuits. Coating them with Glyptal lowered the counting rate of the system by a factor of ten or more, but without changing the ratio of vertical to horizontal counting rate for one train (one directional pair of counting units). The recording circuits were very

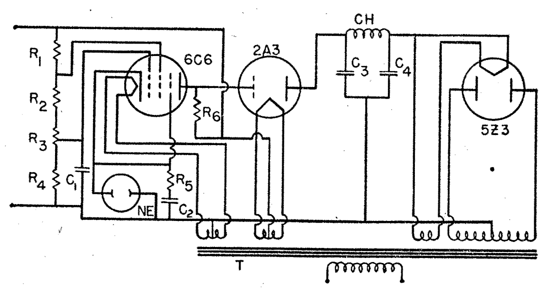

FIG. 5. Typical circuit for power supplies used for mixing and recording circuit.

$R_1 = 10^4$ ohms, 2 watts.
$R_2 = 25{,}000$ ohms, -2 watts.
$R_3 = 15{,}000$ ohms, wire wound potentiometer.
$R_4 = 5000$ ohms, 1 watt.
$R = 50{,}000$ ohms, 1 watt.
$R_6 = 250{,}000$ ohms, 1 watt.
$C_1 = 0.002$ f, tubular.
$C_2 = 0.01$ f, tubular.
$C_3 = C_4$ 16 f, electrolytic.
Ch = Thordarson choke, T-74C29.
T = Thordarson, T-13R08.
(For power tube plate power supply: Ch-T-74C29, T-13R09).

inefficient with neon lamps in darkness (normally they always received a little light at night from the light used in conjunction with the camera).

This difficulty was met by the direct method of putting extra lamps in the tent which housed the telescope, to provide continuous diffused illumination.

Ambient temperature changes for the cosmic-ray telescope were pronounced, as it was housed

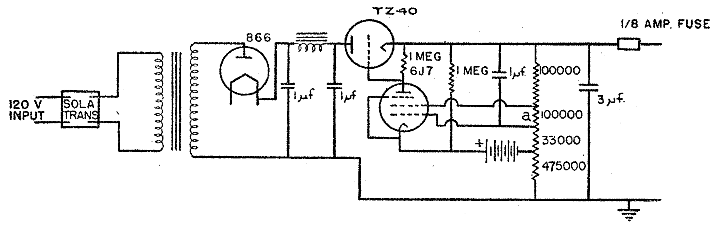

FIG. 6. High voltage power supply with regulator.

in a tent on the open roof of the Physics Building at Washington University. Temperature readings were recorded several times each day. No correlation between temperature and counting rate was discovered for temperatures above 20°F. Any temperature effects should affect all directions uniformly, and corrections were applied to the data to take account of possible aberrations of this type.

III. PROCEDURE

The system was operated continuously, except when the temperature was below 20°F. Every two to eight hours the drum was rotated by hand through two or two-and-one-half degrees; rotations were continuous in the same direction. The meter panel was photographed automatically every half-hour. Since the directional counting arrays are separated in angle by ten degrees, either five two-degree rotations or four two-and-one-half degree rotations provided data covering the complete 180-degree range in zenith angle. This complete coverage was accomplished in periods of from twelve to twenty-eight hours.

The advantages of this manual rotation of the telescope drum over automatic rotation are several, and a summary of these will serve to bring out more information concerning the experimental method used in this work: (1) The functioning of the telescope can be checked at the time of rotation of the drum, which is when unfortunate minor accidents are most likely to occur. (2) The routine calculations, exclusive of finding probable errors, are reduced by lengthening the time intervals during which the drum remains in one position; with automatic rotation this would have been one hour at most. (3) The total time interval for each zenith direction is broken up into subintervals by the automatic photographs, so that one can check the probable error of any point. (4) The number of counts per point on a complete intensity curve is statistically more significant than would be the case if the drum were at one position for only one hour or less. All of these advantages except (1) could be achieved with completely automatic operation of this apparatus if the control circuit were modified to permit the use of other angular intervals and other time intervals.

Whether operated manually or automatically, the present type of apparatus allows the angular interval between successive positions of the drum to be so chosen that each directional array is made to explore one "section"[17] of the zenith angle range. These sections can be joined to form one continuous curve, as described below.

Readings of temperature and atmospheric pressure were recorded several times daily while cosmic-ray observations were carried out.

The data were taken from the photographic record as soon as possible and later reduced as described below.

A few improvements in procedure which this work showed to be desirable are suggested in Appendix III.

IV. TREATMENT OF EXPERIMENTAL DATA

1. Corrections

It was considered advisable to make certain corrections. Since the western end of each section in the east–west curves, for example, begins at the same time, a changing counting rate caused by spurious effects common to the whole instrument (such as voltage changes or ambient temperature changes) could lead to spurious anomalies common to all sections. A good measure of the drift in counting rate is afforded by the total counting rate for all eighteen trains. In the

[17] The word "section" will henceforth, in this paper, be used in this sense, denoting a small portion of the zenith angle range.

absence of spurious effects this total counting rate should be nearly the same for every position traversed by the drum within a ten-degree section. The method of making the corrections, then, involves multiplying each recorded number of counts by such a factor that the total corrected number of counts for each position of the drum is the same and equal to the average total value calculated from the observed totals. The multiplying factors are just the ratios of the various observed total counting rates, one for each position of the drum, to their average value for the given ten degree section. The same factor applies to every one of the eighteen intensities recorded for each position of the drum.

These results of this method of applying corrections are to be noted: (1) Any common bending of the ten-degree sections, which might lead to spurious anomalies, will be straightened in this process. (2) Any directional effects of atmospheric or magnetic disturbances will show up only in the directions actually involved. For the anomalous change in one direction will be a small fraction of the total intensity in that direction, which in turn will certainly not be a large fraction of the total intensity for eighteen directions. (3) These corrections do not eliminate errors in relative intensity between any two sections, caused by different counting rates for different directional arrays. Although the sections can be adjusted to form one continuous curve, as described below, errors can accumulate in this curve in the process of bringing the separate ten-degree sections into coincidence at their terminal points. For a statistical error, say, in one terminal point may be introduced proportionally into every point of the adjacent section. This means that different sections, either before or after being merged into one continuous curve, can be compared with respect to shape but not with respect to intensity; and in particular, that east–west asymmetries cannot be determined from the present data.

2. Adjustment of Sections to Form Complete Curves

The system was rotated through four 2.5° intervals or five 2° intervals to secure data for one curve. Since the individual arrays are separated in angle by ten degrees, sections thus found have common end points. The adjustment of the sections to form a continuous curve involves multiplying each point of a section by that factor which makes one of its terminal points coincide with the terminal point of one adjacent section. The other adjacent section is then similarly matched to this section.

3. Probable Errors

Since automatic recording of meter readings occurred every half-hour, each time interval for one angle is effectively broken into subintervals. From these data one could compute the probable error of every point by usual methods.[18] Since an examination of the data indicated no excessive fluctuations, the labor of such calculations has been omitted. An estimate of the probable error of any point is given by $n^{\frac{1}{2}}$, where n is the number of counts. The statistical treatment described below, moreover, relieves the probable errors of final responsibility for the validity of the results.

4. Statistical Analysis

In order to find time variations in the directional intensity pattern, the daily curves are compared with the time-average of all such curves for the same azimuth. Pearson's criterion for goodness of fit[19] is used. Each ten-degree section of an individual curve is compared with the corresponding section of the time-average curve after the latter has been fitted as follows: Let n_θ be the number of counts per point, at the zenith angle θ, of the time-average curve. Let r_θ be the number of counts per point, at angle θ, of the individual curve. Then

$$\frac{n_\theta}{\sum_{\theta_i}^{\theta_i+10^\circ} n_\theta} \sum_{\theta_i}^{\theta_i+10^\circ} r_\theta = n_\theta'$$

$$(\theta_i = 0^\circ,\ 10^\circ,\ 20^\circ \cdots,\ \text{or } 2^\circ,\ 12^\circ,\ 22^\circ \cdots,\ \text{etc.})$$

gives the points for the time average section fitted to the individual section. The deviation δ_θ

[18] Cf. Gunnar Dahlberg, *Statistical Methods for Medical and Biological Students* (George Allen and Unwin, London, 1940), Chap. VIII; T. C. Fry, *Probability and Its Engineering Uses* (McGraw-Hill Book Company, Inc., New York, 1928).

[19] Discussed by Fry, reference 18, p. 285.

for any point of the individual curve is then

$$\delta_\theta = n_\theta' - r_\theta.$$

Note that

$$\sum_{\theta_i}^{\theta_i+10°} n_\theta' = \sum_{\theta_i}^{\theta_i+10°} r_\theta$$

and

$$\sum_{\theta_i}^{\theta_i+10°} \delta_\theta = 0.$$

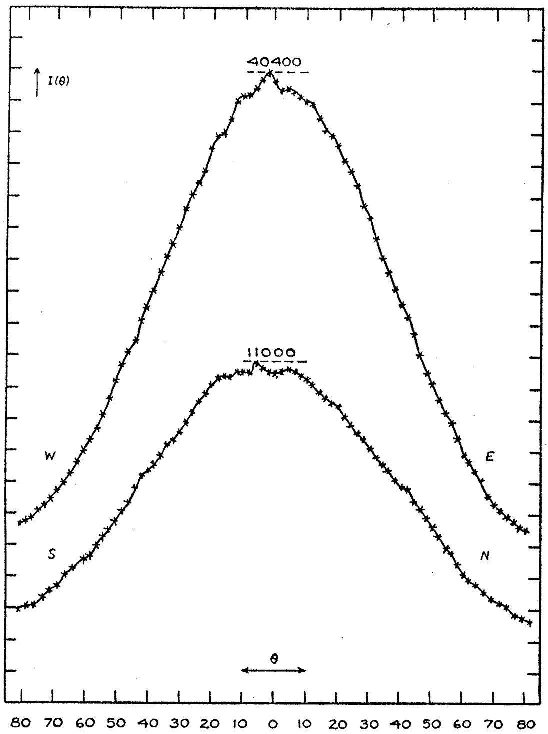

FIG. 7. Time average cosmic-ray directional intensity $I(\theta)$ as a function of zenith angle θ for the E–W azimuth (upper curve) and N–S azimuth (lower curve). For the E–W curve each vertical scale division represents 2000 counts; for the N–S curve each division represents 1000 counts. The maximum intensity for each curve is shown. The time interval covered by the E–W curve extends from 9:10 P.M., March 25, 1943 to 8:10 P.M., April 12, 1943; the time interval for the N–S curve is from 3:35 P.M., April 15, 1943 to 1:06 P.M., April 20, 1943. The average probable error is about 0.4 percent of the maximum intensity for the E–W curve and 0.7 percent of the maximum intensity for the N–S curve.

With the quantity

$$\chi^2 = \sum_{\theta_i}^{\theta_i+10°} \frac{\delta_\theta^2}{n_\theta'},$$

one enters Pearson's table for goodness of fit criteria.[20] The probability number P given by the table is the probability that another run of the experiment would by chance yield a curve deviating from the standard of comparison as much or more than the curve at hand. In the present data each ten-degree section of a curve contains either five or six points; one therefore enters Pearson's table with n'^{20} equal to four or five, respectively, since a relationship between the points is implied by the method of fitting the time-average curve to the individual curve.

[20] Karl Pearson, *Tables for Statisticians and Biometricians* (Cambridge University Press, London, 1930), third edition, Part I, p. 26.

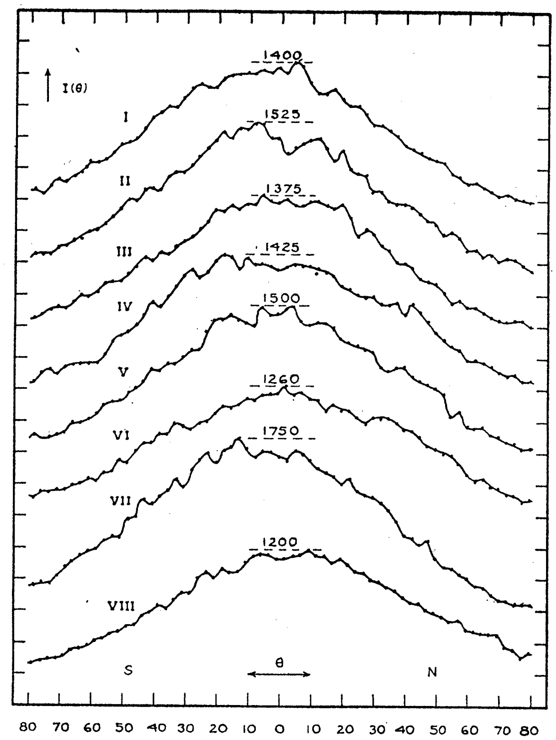

FIG. 8. Individual short-time directional intensity curves for the north–south azimuth. Each vertical scale unit represents 250 counts. The maximum intensity is shown for each curve. The average probable error is about 2 percent of the maximum intensity. The time intervals are as follows (all dates for 1943): I. 4–15, 3:35 P.M. to 4–16, 6:06 A.M. II. 4–16, 9:06 A.M. to 4–16, 7:06 P.M. III. 4–16, 11:36 P.M. to 4–17, 3:06 P.M. IV. 4–17, 3:36 P.M. to 4–18, 1:36 A.M. V. 4–18, 3:36 A.M. to 4–18, 7:36 P.M. VI. 4–18, 8:36 P.M. to 4–19, 8:36 A.M. VII. 4–19, 4:36 P.M. to 4:20, 2:36 A.M. VIII. 4–20, 3:06 A.M. to 4–20, 1:06 P.M.

V. RESULTS AND DISCUSSION

1. The Time-Average Directional Intensity Curves

For the east–west and north–south azimuths the cosmic-ray intensity $I(\theta)$ is plotted as a function of zenith angle θ in Figs. 7–9. The two

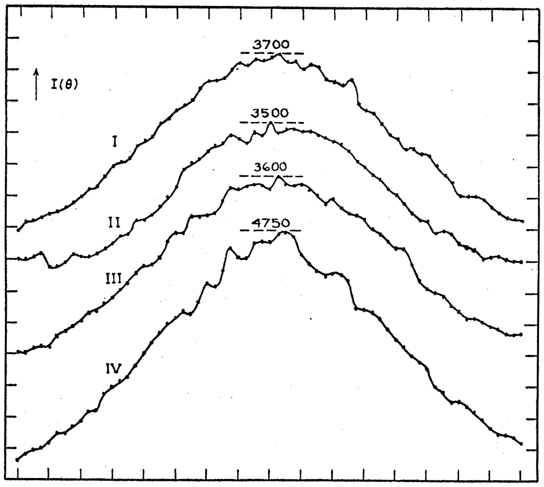

FIG. 9A.

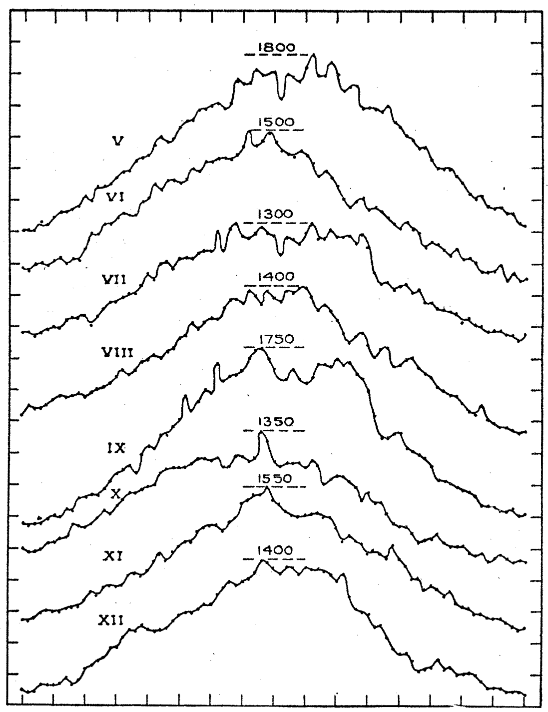

FIG. 9B.

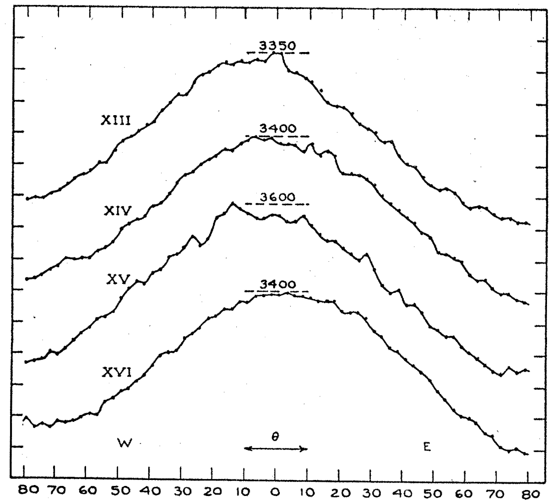

FIG. 9C.

FIGS. 9A–C. Individual directional intensity curves for the east–west azimuth. Each vertical scale unit represents 500 counts for curves I–IV and XIII–XVI, and 250 counts for curves V–XII. The maximum intensity for each curve is shown. The average probable error is about 1 percent of the maximum intensity for curves I–IV and XIII–XVI, and about 2 percent of the maximum intensity for curves V–XII. The time intervals are as follows (all dates for 1943): I. 3–25, 9:10 P.M. to 3–27, 1:10 A.M. II. 3–27, 2:40 A.M. to 3–28, 6:40 A.M. III. 3–29, 4:40 P.M. to 3–30, 7:10 P.M. IV. 3–30, 7:10 P.M. to 3–31, 9:10 P.M. Each of curves V, VII, IX, and XI covers 12 hours starting at 7 P.M. on 3–31, 4–1, 4–2, 4–3, respectively. Curves VI, VIII, X, and XII are for 12-hour periods starting at 7 A.M. on 4–1, 4–2, 4–3, 4–4, respectively. XIII. 4–7, 3:10 A.M. to 4–8, 8:10 A.M. XIV. 4–8, 11:40 A.M. to 4–10, 12:10 A.M. XV. 4–10, 9:40 A.M. to 4–11, 12:10 P.M. XVI. 4–11, 5:10 P.M. to 4–12, 8:10 P.M.

curves of Fig. 7 are summation, or time-average, curves representing all of the data recorded for the E–W and N–S azimuths, respectively; they are obtained by the superposition of the short-time curves of Figs. 8 and 9, which will be discussed in succeeding sections.

These time-average curves are similar in scope to the measurements made previously by Ribner[21] and Cooper[22] in Missouri, although more cosmic-ray counts are recorded here than in the earlier work. This permits a comparison of the present results with those previously reported.

In the present time-average curves prominences can be recognized near E 5°, E 10°, E 20°, W 5°, W 10°, W 20°, S 5°, S 10°, S 20°, and N 5°. At N 20°, where others have reported an anomaly, a prominence is just perceptible. Prominences at 40° in the north, south, east, and west are not strong but are sufficiently evident to bear out the earlier reports that anomalies do exist at these angles. In addition to the 40° anomaly, the data of Ribner and Cooper reveal prominences near 7° and 20° in the E and W azimuths (Ribner and Cooper) and in the N, S, NE, NW, SE, and SW azimuths (Cooper). The prominences in the

[21] See reference 5.
[22] See reference 6.

present curves near 5° and 10° are probably the same as appeared to be one near 7° from the more widely spaced points of the earlier work. The prominences at 20° in the N, S, E, and W appear to be the same for both the present and past data.

The present time-average curves, therefore, tend to confirm rather completely the existence and circular symmetry of the anomalies previously reported; they support the interpretation suggested at that time for this circular symmetry, namely, that lines or bands exist in the primary energy spectrum.[23]

2. The Daily Curves and Their Time Variations

Each of the twenty-four curves of Figs. 8 and 9 spans a period of from twelve to twenty-eight hours, and covers the full 180° of one azimuth at 2° or 2.5° intervals. An attempt was made to determine the existence and character of time variations in the directional cosmic-ray intensity merely from an inspection of these daily curves. This rather obvious step was found inadequate to provide any consistent interpretation of the data; selected combinations of these curves were similarly uninformative.

A better approach to the study of these curves is a section by section comparison of corresponding ten-degree angular intervals of the different curves;[24] this is best accomplished by a statistical analysis. The method adopted has already been described in Section IV, 4, and the results of this analysis will now be discussed.

For the east–west azimuth, Table I gives the probability values P describing the goodness of fit of each ten-degree section of the individual directional intensity curves with the time-average curve; Table II lists the corresponding values for the north–south azimuth. There are many entries for $P \lesssim 0.1$ and, in the E–W azimuth, even for $P \lesssim 0.01$. In determining whether these low values actually indicate significant time variations, three interrelated questions are to be dealt with: (1) A few low P values are to be expected just by chance; is the number of these values here so high as to imply the existence of real time variations? (2) What limiting value of P shall be considered useful for distinguishing abnormal sections of the individual curves, and hence for indicating the angular distribution of any moving prominences? (3) Does the angular distribution of the low P values indicate the absence of random instrumental errors?

The curves of Figs. 10 to 16 are helpful for a consideration of these questions, which will be taken up in order.

(1) In each case of Figs. 10 to 13, for the E–W azimuth, the horizontal "chance line" is appreciably below the actual distribution. This line becomes relatively lower, furthermore, as the limiting values of P are decreased from 0.2 to 0.01; the average ratios of chance expectation to actual number of sections are 0.6 for $P \lesssim 0.2$, 0.4 for $P \lesssim 0.1$, 0.3 for $P \lesssim 0.05$ and 0.17 for $P \lesssim 0.01$. The existence of significant time variations in the

[23] Cf. references 4, 6, and 7.

[24] For this purpose the original corrected data for the individual ten-degree sections are used, rather than the adjusted values which form the continuous curves of Figs. 8 and 9.

TABLE I. Probability values P describing the goodness of fit of the individual east–west curves with their time average.*

Curve / Angular section	I	II	III	IV	V	VI	VII	VIII	IX	X	XI	XII	XIII	XIV	XV	XVI
W 90–80	0.11	0.78	0.50	0.70	0.44	0.87	0.50	0.83	0.22	0.90	0.70	0.53	0.88	0.30	0.92	0.86
80–70	.08	.56	.16	.13	.16	.48	.50	.28	.36	.57	.80	.35	.10	.90	.46	.02
70–60	.91	.10	.0011	.66	.49	.08	.62	.04	.018	.019	.70	.04	.68	.45	.05	.05
60–50	.54	.18	.22	.27	.35	.06	.0012	.97	.50	.70	.11	.46	.52	.02	.54	.08
50–40	.84	.38	.28	.80	.93	.65	.35	.40	.04	.13	.36	.85	.85	.70	.025	.33
40–30	.76	.42	.32	.32	.36	.13	.14	.54	.62	.46	.35	.74	.64	.45	.64	.52
30–20	.56	.011	.21	.30	.94	.65	.30		.25	.82	.88	.23	.86	.38	.0004	.50
20–10	.58	.56	.08	.018	.24	.75	.00008	.25	.03	.30	.40	.30	.10	.29	.001	.50
10–0	.58	.06	.74	.66	.00005	.30	.80	.58	.04	.10	.64		.48	.66	.30	.93
E 0–10	.10	.60	.06	.15		.57	.003	.10	.68	.86	.55	.96	.20	.98	.25	.52
10–20	.38	.45	.74	.56	.30			.08	.00004	.93	.83	.013	.08	.04	.82	.36
20–30	.00001	.84	.16	.04	.34	.10	.05			.035	.75	.12	.26	.21	.04	.33
30–40	.28	.92	.54	.20	.15	.40	.28	.047	.18		.12	.00004	.018	.80	.10	.56
40–50	.0014	.62	.035	.10	.72	.09	.40	.14	.49	.15	.36		.025	.97	.06	.88
50–60	.41	.12	.62	.05	.78	.17	.60	.42	.67	.047	.55	.07		.18	.76	.06
60–70	.0024	.19	.08	.88	.52	.12	.32	.0025	.53	.49	.85	.16	.74	.07	.10	.05
70–80	.21	.48	.84	.68	.044	.0012	.40	.05	.59	.96	.73	.64	.024	.30	.0003	.0002
80–90	.50	.72	.95	.49	.32	.75	.50	.20	.19	.90	.08	.37	.035	.33	.44	.08

* The missing entries for this table represent data thrown out because of instrumental errors.

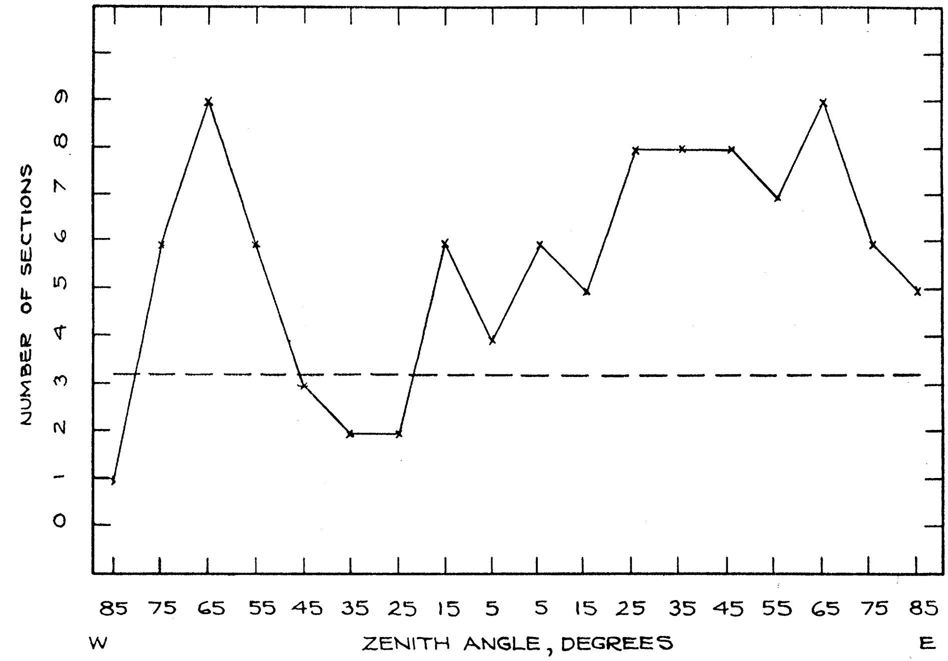

FIG. 10. Number of 10° sections of individual E–W directional intensity curves for which $P \lesssim 0.2$, as a function of zenith angle. The broken horizontal "chance line" shows the most probable number expected by chance for any 10° interval.

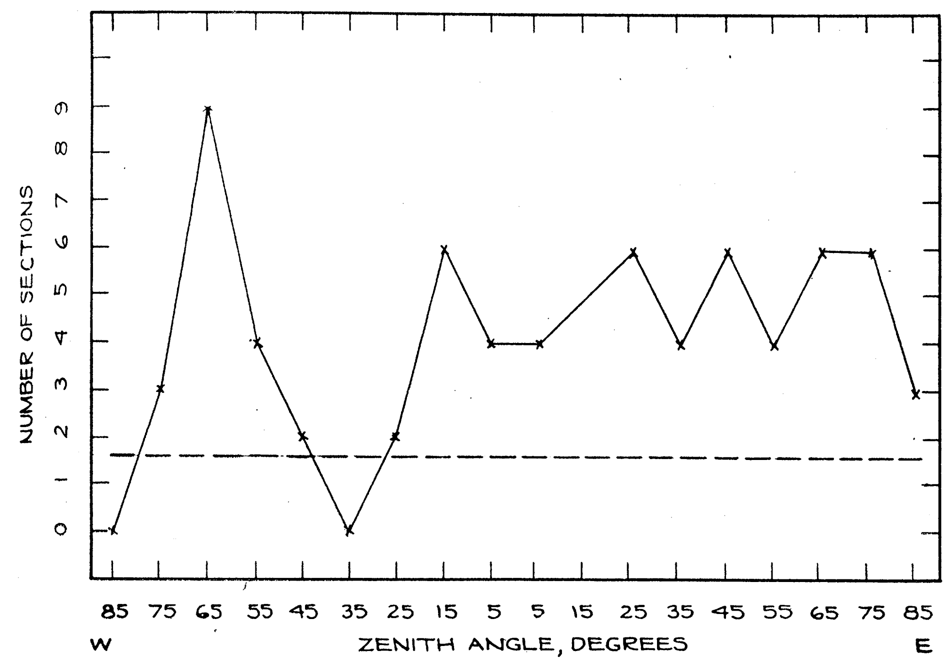

FIG. 11. Number of 10° sections of individual E–W directional intensity curves for which $P \lesssim 0.1$, as a function of zenith angle. The broken line shows the most probable number expected by chance for any 10° interval.

east–west directional intensity pattern therefore seems to be indicated, provided only that random instrumental errors can be shown to be absent.

The results for the north–south azimuth are

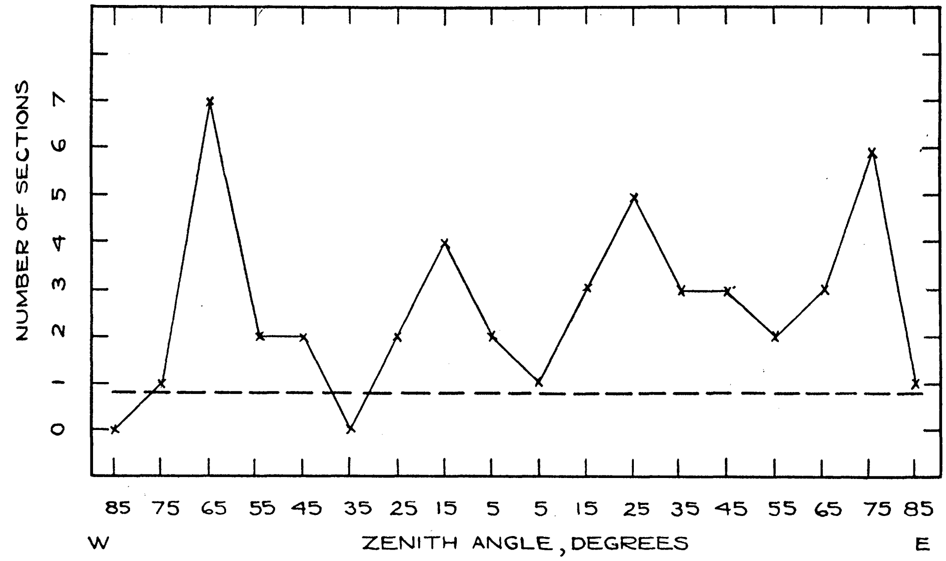

FIG. 12. Number of 10° sections of individual E–W directional intensity curves for which $P \lesssim 0.05$, as a function of zenith angle. The broken line shows the most probable number expected by chance for any 10° interval.

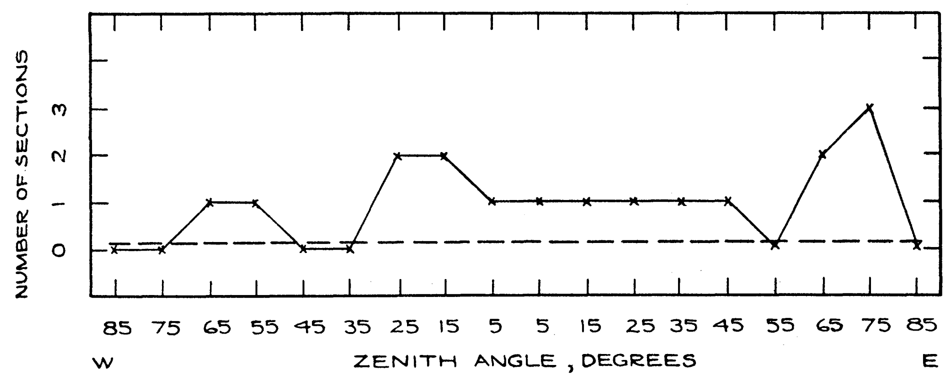

FIG. 13. Number of 10° sections of individual E–W directional intensity curves for which $P \lesssim 0.01$, as a function of zenith angle. The broken line shows the most probable number expected by chance for any 10° interval.

different. For $P \lesssim 0.2$ and $P \lesssim 0.1$ the number of sections is in no case appreciably greater than could be expected by chance (cf. Figs. 15 and 16). Only two sections exhibit a value less than 0.05, although seven would be the normal chance expectation; none has $P \lesssim 0.01$. This situation will be discussed further after questions (2) and (3) have been taken up. For the moment we merely point out this difference between the data for the N–S and E–W azimuths, a difference which implies that time variations of a type which can be revealed by Pearson's test exist in the E–W azimuth but not in the N–S azimuth.

(2) It is reasonable to use the plot of $P \lesssim 0.05$ as a guide in locating the angular distribution of time-varying sections of the pattern. This choice can be justified to some extent by the ratio of the number of sections expected by chance to have $P \lesssim 0.05$, to the number actually observed, for the E–W azimuth (cf. Fig. 12). The average value of this ratio is 0.3 and even lower values exist for several angles, the minimum being 0.11. The corresponding ratio (average value equals 0.17) for $P \lesssim 0.01$ of course does not preclude 0.01 as an upper limit of P, but the observed number of sections for this case is too small to be useful.

(3) The angular distribution for $P \lesssim 0.05$ in the E–W azimuth suggests that instrumental

errors are relatively insignificant. For low P numbers caused by instrumental aberrations may be expected to show a rather uniform angular distribution. This is not the case in the present data, as shown by Fig. 12. Of particular importance are the 80°–90° sections, where the "accidental" counting rate of the telescope should contribute the greatest relative intensity. Of thirty-two sections for this range, only one exhibits a $P<0.05$; none a $P\lesssim 0.01$. That instrumental errors are unimportant is further indicated by the absence in the north–south data of many low P numbers.

We return now to the discussion of the differences between the N–S and E–W observations. It is important to know if this difference is a real cosmic-ray effect or if it can be accounted for by limitations in the experimental or analytical procedure.[25] These possibilities must be considered: (1) That the total time interval covered by the N–S data did not include magnetic or barometric changes like those which occurred while the E–W observations were made. (2) That, in view of the smaller number of curves for the N–S azimuth, there should be effectively a fractional increase in the number of constraints[26] pertaining to these data in the application of Pearson's test; for an implicit relationship between the reference (normalized time-average) curve and any individual short-time curve exists, since the reference curve is an average of all of the individual curves. (3) That a real difference in

[25] A re-examination of the data by another statistical method is desirable, but up to the date of this writing there has been no time for this. In a forthcoming paper by Schremp and Yeater, however, reference will be made to the results of this second analysis, which will have been carried out by then.

[26] The number of constraints for a section in either azimuth has been taken as one; this constraint enters because the total number of counts in the reference section is made equal to the total number in the section being tested for a time variation. "Constraint," in the sense implied here, is defined in Fry, reference 18.

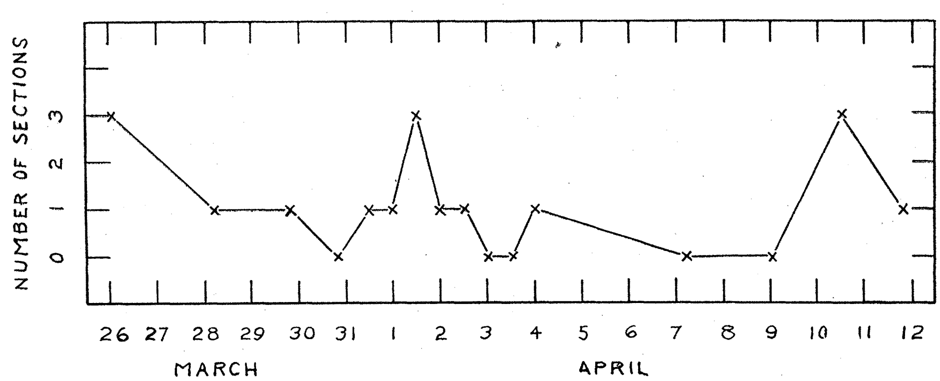

FIG. 14. Time distribution of the 10° sections, of individual E–W curves, for which $P\lesssim 0.01$. The time of day indicated for each date is noon.

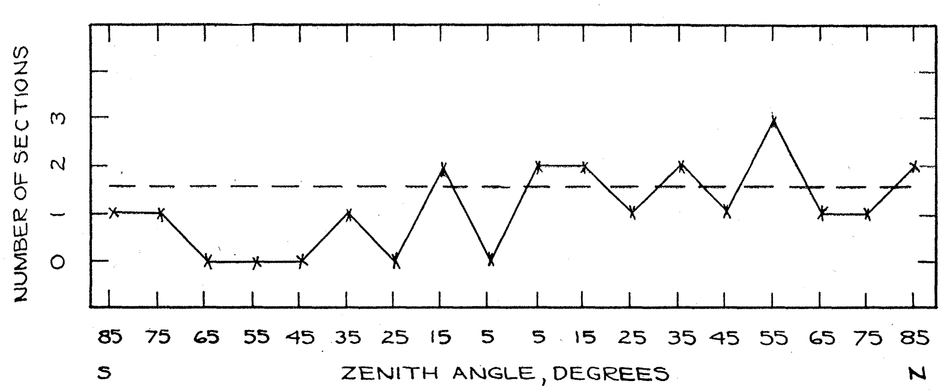

FIG. 15. Number of 10° sections of individual N–S directional intensity curves for which $P\lesssim 0.2$, as a function of zenith angle. The broken horizontal "chance line" shows the most probable number expected by chance for any 10° interval.

the nature of the time variations in the cosmic-ray directional intensity distribution exists between the N–S and E–W azimuths. All of these possibilities will now be examined.

(1) The complete time interval for the eight N–S curves includes five days as against eighteen days, March 25 to April 12, 1943, for the sixteen E–W curves. During these five days, from April 15 to April 20, 1943, the international magnetic character numbers (cf. Fig. 17) show no exceptional uniformity; no general difference between the magnetic fluctuations associated with the N–S and E–W cosmic-ray data is revealed. There is the particular difference, however, that no magnetic disturbances severe enough to be classed as storms occurred between April 15 and April 20; while three brief storms between March 23 and April 12 were reported by some of the stations making magnetic observations.[27] As to the atmospheric pressure, the barometer readings at St. Louis for the period April 15 to April 20 show a somewhat more stable condition than existed at several times during the preceding month (cf. Fig. 17). A change of pressure amounting to 0.6 cm Hg did occur, however, while the N–S cosmic-ray data were taken; the changes were not more than 1.0 cm throughout most of the time for the E–W data.

The possibility exists, therefore, that the N–S results may be caused by the somewhat more quiescent conditions of the magnetic field and/or atmospheric pressure; but the evidence favoring this possibility is not entirely convincing. For the

[27] Terr. Mag. 48, 117, 188 (1943).

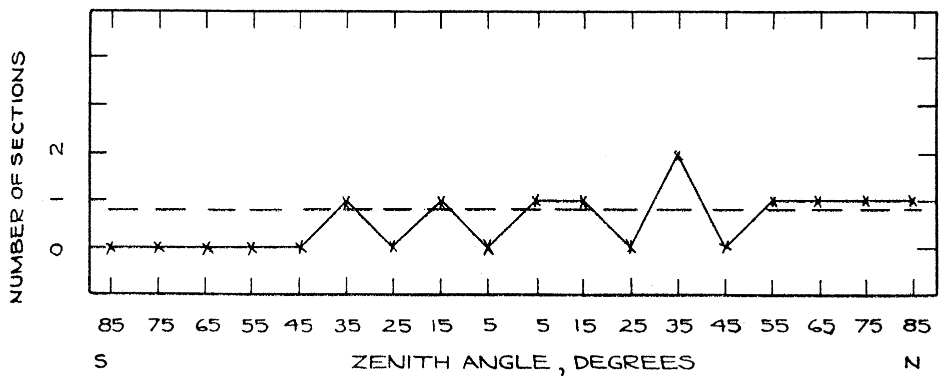

FIG. 16. Number of 10° sections of individual N–S directional intensity curves for which $P \lesssim 0.1$, as a function of zenith angle. The broken line shows the most probable number expected by chance for any 10° interval.

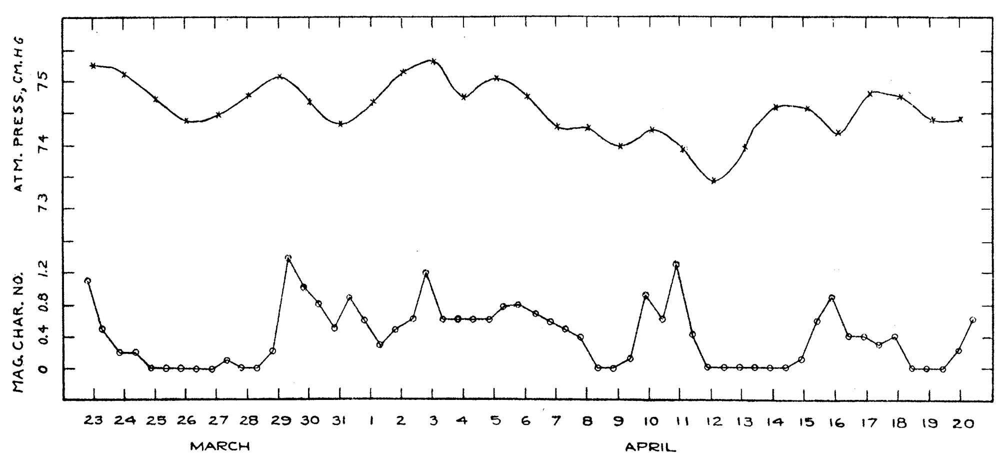

FIG. 17. Variation of atmospheric pressure at St. Louis and of international magnetic character number, for the time covered by the present cosmic-ray data. The time of day indicated for each date is noon. The scale of ordinates for each curve is given at the left.

difference between the N–S and E–W cases, with regard to magnetic and barometric conditions, is not great.

(2) Even if we take the somewhat extreme steps of increasing the number of constraints for the N–S case only, and letting this increase equal one, the difference between the N–S and E–W results is not removed. In this case an entry of $P \lesssim 0.1$ in Table II becomes $P \lesssim 0.05$; Fig. 16 then becomes a graph of $P \lesssim 0.05$, with the height of the "chance line" reduced from 0.8 to 0.4. For this assumed condition the average ratio of chance expectation to observed value for the number of sections with $P \lesssim 0.05$ is 0.72, and also for $P \lesssim 0.01$ it is 0.72, with no entries for $P \ll 0.01$; these are to be compared to values of 0.3 and 0.17, respectively, for the corresponding ratios in the E–W case, where in addition P values lower than 0.0001 are found (Table I).

From this it appears that the difference in the present results for the N–S and E–W azimuths has its origin in some physical circumstance.

(3) This possibility, that the character of the time variations in the cosmic-ray directional intensity patterns is a function of azimuth, is not ruled out by the preceding considerations (1) and (2). That time variations in the N–S pattern may be absent is consistent, furthermore, with certain interpretations of the E–W data, as discussed in the next section. This third possibility, in the light of all the evidence, appears by far the strongest.

3. Implications of the Time Variations

One of the purposes of this experiment was to determine whether rapid time variations exist for the anomalies observed in the static cosmic-ray directional intensity pattern. The result of the experiment in this respect is that no significant variations in these anomalies are revealed by the present analysis. On the other hand, this analysis does indicate time variations of an independent character.

The immediate evidence for the independence of the static and dynamic anomalies lies in the fact that the circular symmetry exhibited by the static anomalies is not exhibited by the time variations in the pattern. The fundamental reason for this independence, however, would appear to be that different origins can be ascribed to the two effects. The circularly symmetrical anomalies in the time-average curves have their origin in atmospheric effects, as previously discussed by others.[28] The probable origin of the time variations will be discussed in the following paragraphs.

In the E–W azimuth a dynamic character in the cosmic-ray directional intensity pattern is indicated by Fig. 12 to exist near W 65°, and E 75°, and near W 15° and E 25°. As we shall see, there is reason to believe that these peaks actually represent symmetrical dynamic regions. For if the variations in the pattern which produce the peaks in Fig. 12 really occur at 20° and 70°, respectively, then the observed asymmetry can easily result from a slight inaccuracy in the determination of the vertical direction for the cosmic ray telescope. An error of even a degree or two in this determination[29] can cause a time variation at 20° to appear at 25° on one side and 15° on the other in Fig. 12, and similarly for variations at 70°; for a point at E 25°, for example, means only that the variation in the pattern lies between 20° and 30°. Such an explaining away of the small observed asymmetry of course requires that this asymmetry be in the

TABLE II. Probability values P describing the goodness of fit of the individual north–south curves with their time average.

Curve / Angular section	I	II	III	IV	V	VI	VII	VIII
S 90–80	0.37	0.95	0.86	0.18	0.24	0.62	0.66	0.64
80–70	.64	.32	.66	.14		.50	.50	.85
70–60	.48	.95	.57	.70	.77	.95	.92	.69
60–50	.24	.87	.51	.60	.66	.52	.46	.84
50–40	.91	.60	.33	.65	.89	.27	.24	.60
40–30	.52	.32	.76	.08	.68	.58	.68	.36
30–20	.25	.90	.29	.70	.28	.56	.22	.32
20–10	.85	.52	.84	.17	.74	.52	.49	.06
10–0	.98	.65	.93	.87	.28	.62	.84	.95
N 0–10	.46	.09	.32	.96	.19	.30	.82	.29
10–20	.08	.20	.57	.69	.57	.74	.84	.58
20–30	.64	.18	.62	.41	.74	.26	.56	.97
30–40	.64	.26	.66	.10	.25	.09		.75
40–50	.41	.86	.47	.71	.71	.95	.16	.46
50–60	.41	.29	.17	.58	.027	.45	.49	.18
60–70	.56	.21	.80	.90	.63	.80	.71	.07
70–80	.72	.62	.30	.97	.02	.82	.33	.52
80–90	.91	.68	.08	.18	.69	.88	.92	.56

[28] Cf. references 4, 6, and 7.

[29] The geomagnetic vertical should be used when magnetic effects are discussed, and this is about 3½° to the east of the geographic vertical at St. Louis; the geographic vertical, however, is used for the present data. If the geomagnetic vertical is used, the peaks in Fig. 11 tend to become symmetrical. The experimental alignment of the telescope with the vertical direction was accurate to about 1°.

same direction for both the 20° and 70° cases; this requirement is fulfilled.

Another feature to be noted in Fig. 12 is that the higher peaks occur at the larger angles. The greater tendency to change thus exhibited at the large zenith angle of 70° is an indication that magnetic effects, rather than atmospheric pressure changes, are responsible for these time variations. This follows because variations caused by atmospheric pressure changes should be more pronounced at smaller angles.[30] Variations caused by magnetic changes, as brought out later, are not restricted in this way.

Further evidence that these cosmic-ray time variations are associated with terrestrial magnetic changes comes from the time distribution of the very low values of the probability index P (Fig. 14). It happens that maxima in this curve, centered at March 26, April 1, and April 10, are observed coincident with or just following the occurrence of magnetic disturbances. (Magnetic data are plotted in Fig. 17; the disturbances referred to are listed specifically elsewhere.)[31]

These magnetic changes can affect the directional pattern by distorting the allowed cones of the primary cosmic rays. In considering the effect of changes in these cones we perceive that the absence of time variations in the N–S pattern can be consistent with the hypothesis that variations at other azimuths are caused by magnetic fluctuations.

For directional cosmic-ray changes of magnetic origin must be caused by the movement of an allowed cone boundary across the direction of observation. Now at the magnetic latitude of St. Louis, approximately N 48°, the boundary of the allowed cone is essentially the common boundary of the simple shadow cone and the Störmer cone.[32] The character of this boundary for various energies is shown in Fig. 18.[33] From this we can see how certain of these boundaries can produce the observed dynamic regions in the E–W pattern (at approximately ±20° and ±70°) without intersecting the N–S meridian. At W 20°, for example, lies a cone boundary for a positive particle with an energy slightly greater than 0.2 Störmer. The N–S meridian is in the forbidden region for this energy; hence a movement of this cone can produce no changes in the N–S pattern. The region near E 20° can be similarly described with reference to a negative primary particle. In dealing with the region near E 70° we can invoke the cone for a positive particle with energy of about 0.6 Störmer. In this case the north–south meridian is in the region of full light, and no variations in the N–S pattern are to be expected from changes in this cone. The corresponding cone for a negative particle can account in a similar way for the dynamic character of the pattern near W 70°.

In thus relating the observed time variations with magnetic fluctuations, we have a reasonable explanation of their symmetry in the E–W azimuth and their absence in the N–S azimuth. More than this, we find in the symmetry of these variations a new kind of evidence supporting a conclusion previously advanced by Schremp,[34] to

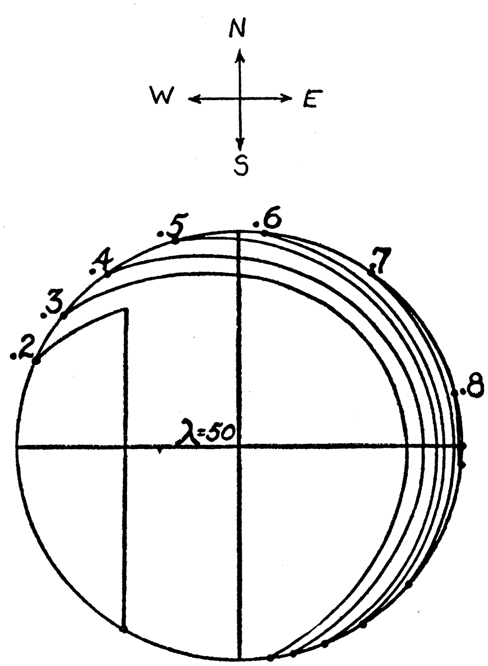

FIG. 18. Simple shadow cones, for positive particles, at geomagnetic latitude north 50°. Energies are in Störmers.

[30] This can be demonstrated as follows: Let h_0 be the vertical height of the atmosphere, and h the atmospheric thickness looking in the direction θ from the zenith. Then to a good approximation

$$h = h_0 \sec\theta \quad \text{or} \quad \cos\theta = h_0/h.$$

Hence

$$(\partial\theta/\partial h_0)_{h=\text{const.}} = -(1/h)\operatorname{cosec}\theta = -(1/h_0)\cot\theta.$$

[31] See reference 27.

[32] Cf. E. J. Schremp, Phys. Rev. **54**, 169 (1938).

[33] Reference 32, Fig. 5.

[34] Cf. reference 7.

the effect that positive and negative particles with the same e/m exist among the primary cosmic rays.

ACKNOWLEDGMENTS

Thanks are expressed especially to Dr. E. J. Schremp, who proposed the problem, for his cooperation during the experimental work and for his help in the preparation of this paper; a particular debt of gratitude is due him for suggesting the statistical analysis and for contributing to the interpretation of the results of this analysis. The encouragement and advice of Professor A. L. Hughes is gratefully acknowledged. The Department of Terrestrial Magnetism of the Carnegie Institution was helpful in supplying terrestrial magnetic data. Construction of the apparatus was financed jointly by Washington University and by grants made to Dr. E. J. Schremp from the Penrose Fund of the American Philosophical Society and from the Rumford Fund of the American Academy of Arts and Sciences.

APPENDIX I

Geiger Counter Construction

The cathode is shown in Fig. 19; this is entirely of brass. The end fittings marked f are used in the vacuum seal. The method of securing this seal is shown in detail in Fig. 19B; R is a gum rubber washer which is compressed against the inner surface of f and around the glass lead-in g to form the seal; the nut N bears on the metal washer W which crushes the rubber. The cathode is formed by hard-soldering the threaded fitting f to the disk d, then soft-soldering d to the light brass cylinder c. The glass lead-in is shown enlarged in Fig. 19C. The complete anode assembly is shown in Fig. 19D.

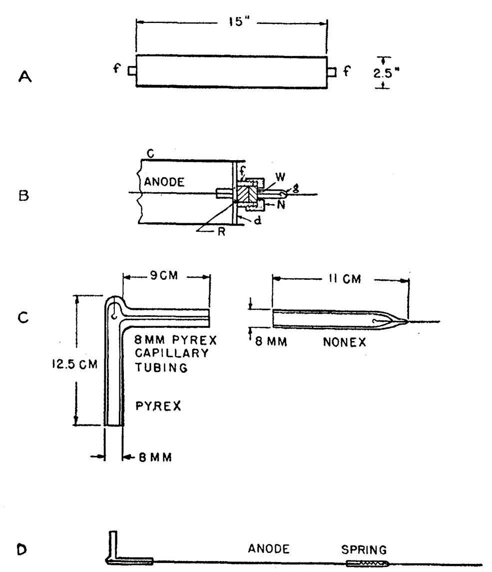

FIG. 19. Structure of the Geiger counters. A, cathode; B, vacuum seal; C, glass lead-ins; D, anode assembly.

The anode is prepared as follows: A length of 0.010″ tungsten wire is cut off and a loop formed at each end by twisting under a tension of about two kilograms; the wire is then rubbed vigorously with fine sand paper. It was not found necessary to flash the anodes in vacuum.

The cathodes are cleaned in an acid solution consisting of about three parts HNO_3 (sp. gr. 1.403), one part H_2SO_4 (sp. gr. 1.84) and twenty parts water. After being washed several times in tap water and in distilled water the cathodes are permitted to stand in air a few days to form a thin oxide layer on the brass.

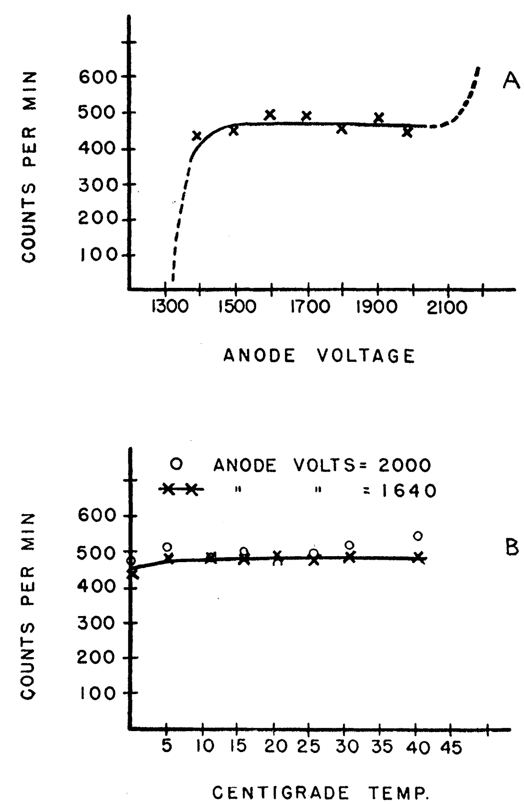

FIG. 20. A, Geiger counter characteristic curve; B, counting rate of Geiger counter at different temperatures.

The filling gas mixture consists of 8 mm alcohol, 4 mm petroleum ether, and 7.8 cm argon. A typical characteristic curve is shown in Fig. 20A. The effect of temperature on the counting rate of an early test counter is shown in Fig. 20B.

APPENDIX II

Pulse Cable Connection

The manner in which the counter pulses are properly distributed to the mixing circuits is indicated in Fig. 21 and Fig. 22. Figure 21 is a simplified diagram showing the interconnections for just two of the eighteen directions. From each quenching unit a shielded cable runs one-fourth of the way around the drum on either side, and from these cables the pulses are tapped off to the coincidence circuits. The mixing circuits for the direction indicated by the broken lines are represented by the ten small dots at the left, while for the direction defined by the full lines the mixing circuits are at the right. Counter units A and A' feed into vacuum tubes a_1 and a_1'; similarly B and B' feed into b_1 and b_1', etc. In order to interconnect thirty-six counter units for eighteen directions this system is simply extended; one cable from each counter unit runs halfway around the drum and pulses are tapped off at the appropriate mixing-recording panel. The complete wiring diagram for this is given in Fig. 22.

APPENDIX III

Suggested Improvements In Apparatus and Procedure for Cosmic-Ray Directional Intensity Measurements

(1) The general circuit arrangement of the multidirectional telescope is satisfactory, but a recording circuit not using neon lamps should be employed.

(2) The "fast" type of Geiger counter containing organic vapor is not good for this work because of limited life.

(3) The cosmic-ray telescope should be operated in a shack in which constant conditions of temperature and illumination can be maintained.

(4) An output pulse length, for the Geiger counter-quenching circuit combination, of the order of a microsecond should be achieved, in order to reduce the "accidental" counting rate. This, it is believed, can be done by adjustment of constants in the quenching circuit; a resulting excessive decrease in pulse size can be compensated by another amplifier stage. This seems more practicable than a triple coincidence counting system, for the present type of apparatus.

(5) Observations should be made in rapid alternation in the N–S and E–W azimuths (or any other pair at right angles to each other) so that in effect patterns for both azimuths are recorded simultaneously.

(6) If measurements like those described in this paper are made, a second telescope operating at fixed zenith angles should be run concurrently, giving direct readings of intensity *versus* time for various angles. If possible, ionization chamber measurements of total intensity should be carried along at the same time.

(7) A high angular resolution, of three degrees or less, with respect to zenith angle, is desirable for a cosmic-ray telescope used in tracing the fine structure; for a more precise knowledge of this pattern, which would immeasurably facilitate the interpretation of the data, appears to be easily attainable by this means. A second telescope used for direct observation of time variations at fixed angles would preferably have a resolution in zenith angle equal to the angular spacing between the directional trains, in the present case ten degrees.

APPENDIX IV

Notes on Control Circuit

These notes pertain to Fig. 2. In reference 13 is given a description of the manner of starting the motor M (which causes the drum to rotate) at optional time intervals of

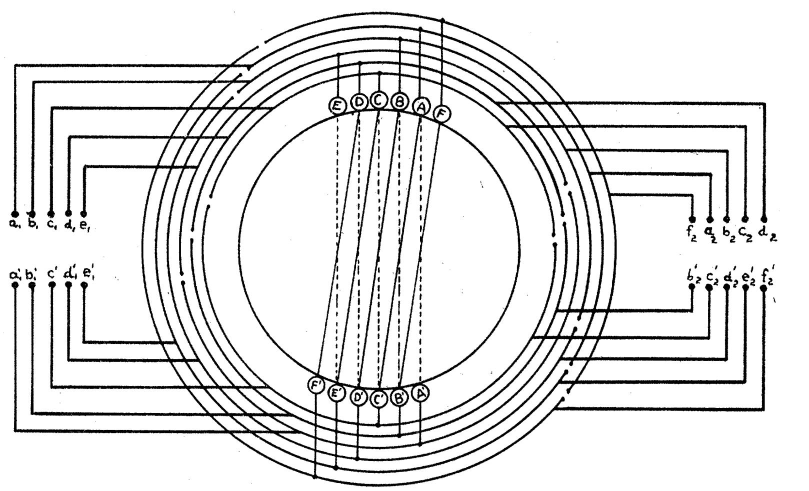

FIG. 21. Pulse cable connections for two directions of observation. The dots marked with lower case letters represent mixing tubes in the recording circuit. Circles marked with capital letters represent Geiger counter units. The angular separation of these two directions is 10°.

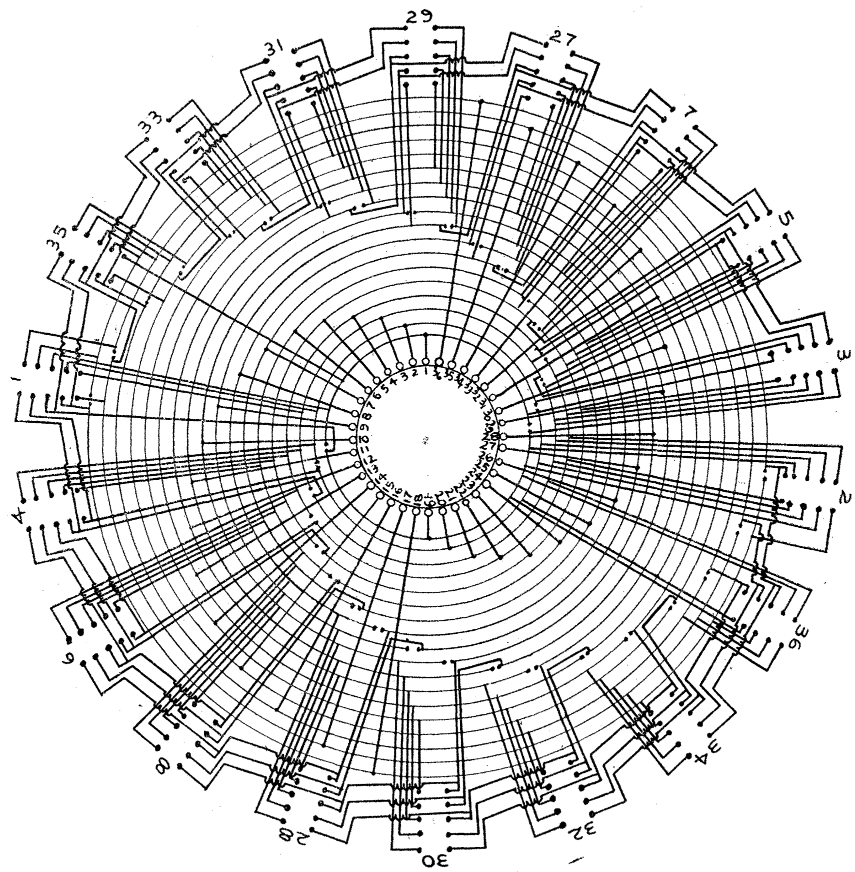

FIG. 22. Complete pulse cable connections for the multidirectional cosmic-ray telescope. The Geiger units are numbered *1* to *36* around the inner circle. The cables are shown as concentric semicircles. Every group of dots represents one panel of mixing tubes. Each group is assigned the number of one of the Geiger units of the center train for that direction; for example, group 1 represents the mixing-recording circuit for the complete directional array of counters which includes the following units in double-coincidence trains: *3* and *17*, *2* and *18*, *1* and *19*, *36* and *20*, *35* and *21*.

twenty minutes, thirty minutes, or one hour, and of the way in which the motor is stopped after it has experienced a predetermined number of revolutions. This number, and hence the angle through which the drum is rotated, is chosen by selector switch Sw_2. At the position 2 of Sw_2, relay 2 will operate, and hence the motor will stop, every time either pair of contacts a or d of Sw_3 is shorted by the rolling contact* which is driven by M through reducing gears. This gear ratio is so adjusted that for a six degree rotation of the drum the rolling contact passes once over every set of contacts a to f, and these sets are spaced sixty degrees apart. Hence for the setting 2 of Sw_2 the motor is stopped after every three-degree rotation of the drum. Similarly, for setting 1 the motor is stopped whenever any set of contacts a to f is shorted, or for every one degree rotation of the drum. Setting 3 of Sw_2 stops the rotation of the drum after six degrees.

When relay 2 and simultaneously relay 4 are activated, thereby stopping the motor, the coils MR and L are energized. MR is the coil of a message register which counts the number of small rotations of the drum and hence indicates the angular position of the drum at any time during a run of the experiment. L is a solenoid which trips a camera and causes a photographic record of the meter panel to be made.

The camera can be tripped automatically by the clock switch without any rotation of the drum. This occurs if Sw_4 is at position 2.

Switch Sw_1 is a push-button switch by means of which the clock switch can be shorted by the operator, thereby enabling him to start the motor M or, if Sw_4 is at 2, to take a picture of the meter panel, at any arbitrary time.

* Cf. reference 13.

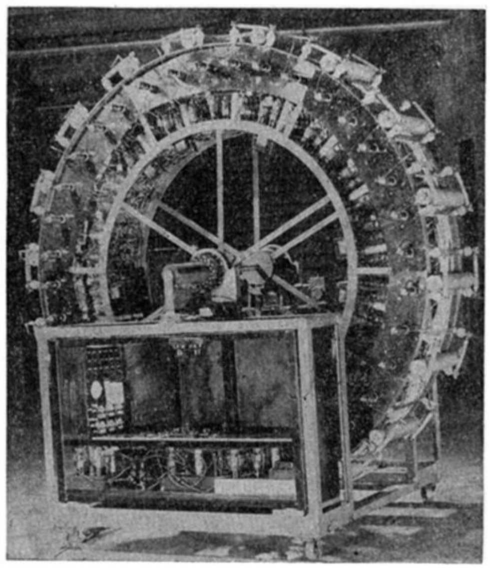

FIG. 1. Multidirectional cosmic-ray telescope. At the time this picture was taken only eighteen of the seventy-two Geiger counters were in position on the drum.